[Electronic Supplementary Information to accompany *J. Am. Chem. Soc.* manuscript ja405495u]

Enhanced Catalytic Activity through the Tuning of Micropore Environment and Supercritical CO_2 Processing: Al(porphyrin)-based Porous Organic Polymers for the Degradation of a Nerve Agent Simulant

Ryan K. Totten, Ye-Seong Kim, Mitchell H. Weston, Omar K. Farha,* Joseph T. Hupp,* SonBinh T. Nguyen*

Department of Chemistry and the Institute for Catalysis in Energy Processes, Northwestern University, 2145 Sheridan Road, Evanston, Illinois 60208-3113, USA

Email: o-farha@northwestern.edu (O.K.F.), j-hupp@ northwestern.edu (J.T.H.), and stn@northwestern.edu (S.T.N.)

Table of Contents *Page number*

S1. General information. ^{1}H and ^{13}C NMR spectra were recorded on a Bruker Avance 500 (499.4 MHz for ^{1}H, 125.8 MHz for ^{13}C) spectrometer. ^{1}H NMR data are reported as follows: chemical shift (multiplicity (bs = broad singlet, s = singlet, d = doublet, t = triplet, q = quartet, and m = multiplet), coupling constant and integration). ^{1}H and ^{13}C chemical shifts are reported in ppm downfield from tetramethylsilane (TMS, δ scale) using the residual solvent resonances as internal standards.

^{1}H-^{13}C cross-polarization, magic angle spinning (CP-MAS) nuclear magnetic resonance spectra were recorded on a Varian VNMRS 400 MHz (400 MHz for ^{1}H, 100. MHz for ^{13}C) spectrometer (Varian, Inc., Palo Alto, CA, USA) equipped with a 5-mm HXY T3 PENCIL probe. The samples were packed into a standard 5-mm (external diameter) zirconia rotor with a volume of 160 μL and capped with a Teflon spacer. The spinning rate was at 10 kHz. ^{13}C NMR chemical shifts are reported in ppm downfield relative to tetramethylsilane (TMS) as zero ppm, calibrated using adamantane (38.3 ppm) as a secondary standard. All the spectra were acquired with neat powdered samples at room temperature. All the data were processed by VnmrJ software (Varian, Inc., Palo Alto, CA, USA) with a line broadening of 20 Hz.

Matrix-assisted laser desorption ionization time-of-flight (MALDI-ToF) mass spectra were recorded on a Bruker Autoflex III spectrometer using reflective positive MALDI ionization method. Sample was typically prepared by mixing a solution of the material with pyrene matrix on the MALDI plate and allowing the spot to dry before analysis.

UV-vis spectra were obtained in $CHCl_3$ or MeOH on a Varian Cary 500 spectrophotometer and the absorption of *p*-nitrophenol was monitored at λ_{max} = 311 nm.

Elemental analyses were provided by Atlantic Microlab, Inc. (Norcross, GA). Thermogravimetric analysis (TGA) experiments were performed on a Mettler Toledo TGA/SDTA851 interfaced with a PC using Star software. Samples were heated at a rate of 10 °C/min under a nitrogen atmosphere.

Inductively coupled plasma optical emission spectroscopy (ICP-OES) was conducted on a Varian Vista MPX ICP- OES instrument that is equipped to cover the spectral range from 175 to 785 nm. Samples (3 mg) were digested in conc. H_2SO_4:30% aq H_2O_2 (3:1 v/v) and heated at 120 °C until the solution became clear and colorless. The clear solution was diluted to 5% with deionized H_2O and analyzed for Al (308.215 nm) content against standardized solutions containing 2, 5, 10, 20, and 30 ppm of Al that were prepared from a commercially available ICP standard solution.

All adsorption and desorption measurements were performed on a Micromeritics Tristar 3020 (N_2) system (Micromeretics, Norcross, GA) and measured at 77 K. Between 40-100 mg of samples were employed in each

measurement and the data were analyzed using the ASAP 2020 software (Micromeretics, Norcross, GA). Before measurements, thermally activated samples were degassed for 12 h at 150 ºC under high vacuum (< 10^{-4} bar). For the supercritical CO_2 processed samples, the samples were degassed under vacuum for an extra ½ h prior to measurements (the standard degas period on the Tristar 3020 instrument was 30 minutes). The specific surface areas for N_2 were calculated using the Brunauer-Emmet-Teller (BET) model in the range of $0.01 < P/P_0 < 0.1$ for type I isotherms and $0.01 < P/P_0 < 0.2$ for type II isotherms. The pore size distributions were calculated from the adsorption-desorption isotherms by density functional theory (DFT) in the range of $5.0 \times 10^{-5} < P/P_0 > 0.95$. The pore size distributions obtained were calculated using the slit-pore NLDFT model.

MeOH vapor sorption isotherms were performed at 25 °C on a VTI MB-300G Gravimetric Analyzer (VTI Corp., Hialeah, FL, USA). All samples (5 mg) were degassed at 60 °C under high vacuum (< 10^{-3} bar) for 120 min or until weight equilibration (< 0.0010 wt% change over 5 min). Data was logged at 2 min intervals or every 0.200 wt% change while samples were allowed to equilibrate for ~45 min for each step or < 0.0010 wt% change over 5 min.

Pycnometer measurements were carried out at 25 °C on a Micromeritics AccuPyc II 1340 Pycnometer (Micrometetics, Norcross, GA).

S2. General procedures and materials. All air- or water-sensitive reactions were carried out under nitrogen using oven-dried glassware. All synthetic experiments concerning porphyrin and porphyrin derivatives were carried out under light-deficient conditions: the hood lights were turned off and the reaction flasks are covered with aluminum foil to further minimize light exposure. Isolated porphyrin products were stored at low temperatures (-10 °C) in foil-covered vials. All flash-chromatography was carried out using silica gel (MP Silitech 60-200 mesh) under a positive pressure of nitrogen, unless otherwise noted. Analytical thin layer chromatography (TLC) was performed using glass-backed silica gel 60 F_{254} plates (Merck EMD-571507). Visualization of the TLC results was achieved by observation under UV light (254 nm).

Tetrahydrofuran and dichloromethane (Fisher Scientific) were dried over neutral alumina in a Dow-Grubbs solvent system[S1] installed by Glass Contours (now JC Meyer Solvent Systems, Laguna Beach, CA, USA). All other reagents were purchased from the Aldrich Chemical Company (Milwaukee, WI, USA) and used without further purification, unless otherwise noted. Deuterated solvents were purchased from Cambridge Isotope Laboratories (Andover, MA, USA) and used without further purification. *p*-Nitrophenyl diphenylphosphate (PNPDPP),[S2] 5-pentafluorophenyl dipyrromethane,[S3] and *tetrakis*(4-ethynylphenyl)methane[S4] were synthesized according to published procedures.

S3. Preparation of Al(porphyrin) monomers.

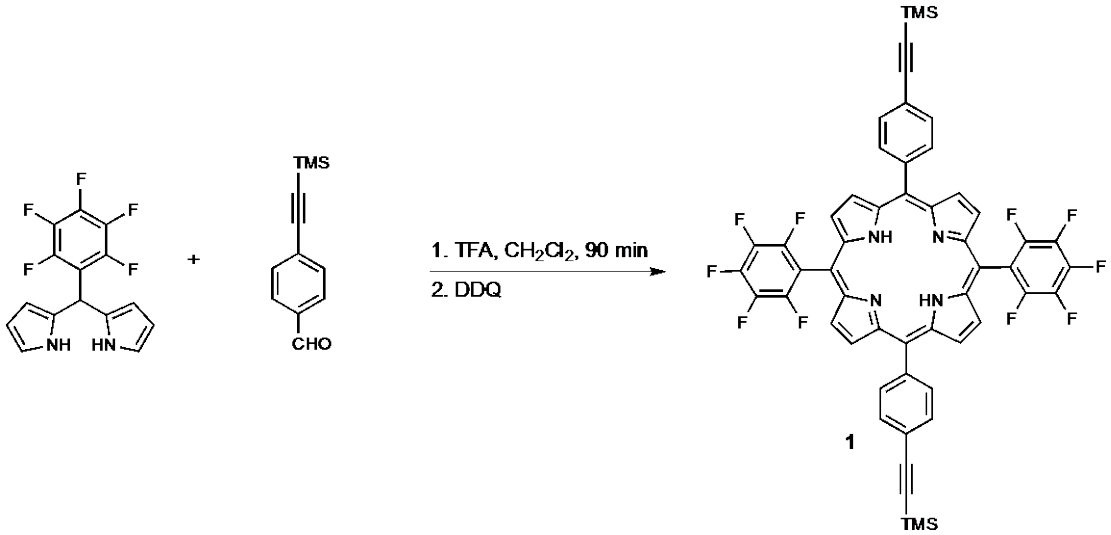

5,15-*Bis*(pentafluorophenyl)-10,20-*bis*[4-[2-(trimethylsilyl)ethynyl]phenyl]porphyrin. This compound was synthesized following a modified literature procedure.[S5] 5-Pentafluorophenyl dipyrromethane (4.8 g, 15.3 mmol) and 4-[(trimethylsilyl)ethynyl]benzaldehyde (3.1 g, 15.3 mmol) were combined with CH_2Cl_2 (1.5 L) in a 3 L round-bottom flask equipped with a magnetic stir bar. The resulting mixture was degassed with N_2 for ten minutes before TFA (2.0 mL, 27.4 mmol) was added. After stirring under N_2 for 1.5 h at room temperature, DDQ (5.2 g, 23.0 mmol) was added as a solid and the resulting mixture was allowed to stir for an additional 1 h. Triethylamine (3.8 mL, 27.4 mmol) was then added and the mixture was allowed to stir for 12 h more before being evaporated to dryness using a rotary evaporator. The remaining crude product was purified by silica gel column chromatography (column dimensions = 60 mm × 250 mm, eluent =

hexanes/CH_2Cl_2 3:1 v/v) to give the desired porphyrin as a purple solid (1.5 g, 1.5 mmol, 20% yield). ^{1}H NMR (499.4 MHz, $CDCl_3$): δ -2.83 (s, 2H, N*H*), 0.40 (s, 18H, Si-(CH_3)$_3$, 7.91 (d, *J* = 8.5 Hz, 4H, Ar-*H*), 8.17 (d, *J* = 8.5 Hz, 4H, Ar-*H*), 8.58 (d, *J* = 4.5 Hz, 4H, β-*H*), 8.93 (d, *J* = 4.5 Hz, 4H, β-*H*). {^{1}H}^{13}C NMR (125.8 MHz, $CDCl_3$): δ 0.2, 96.2, 102.5, 104.8, 120.8, 123.2, 130.7, 134.6, 141.5. MALDI-ToF MS (reflective positive mode): Calcd for $C_{54}H_{36}F_{10}N_4Si_2$: 987.05, found: *m/z* 987.54 [M]$^+$. UV-vis: (nm, (ε ×10^4 /M^{-1}cm^{-1})) 416 (47.5), 512 (1.5), 545 (0.3), 588 (0.5), 642 (0.2). See Figure S1 for the NMR spectra.

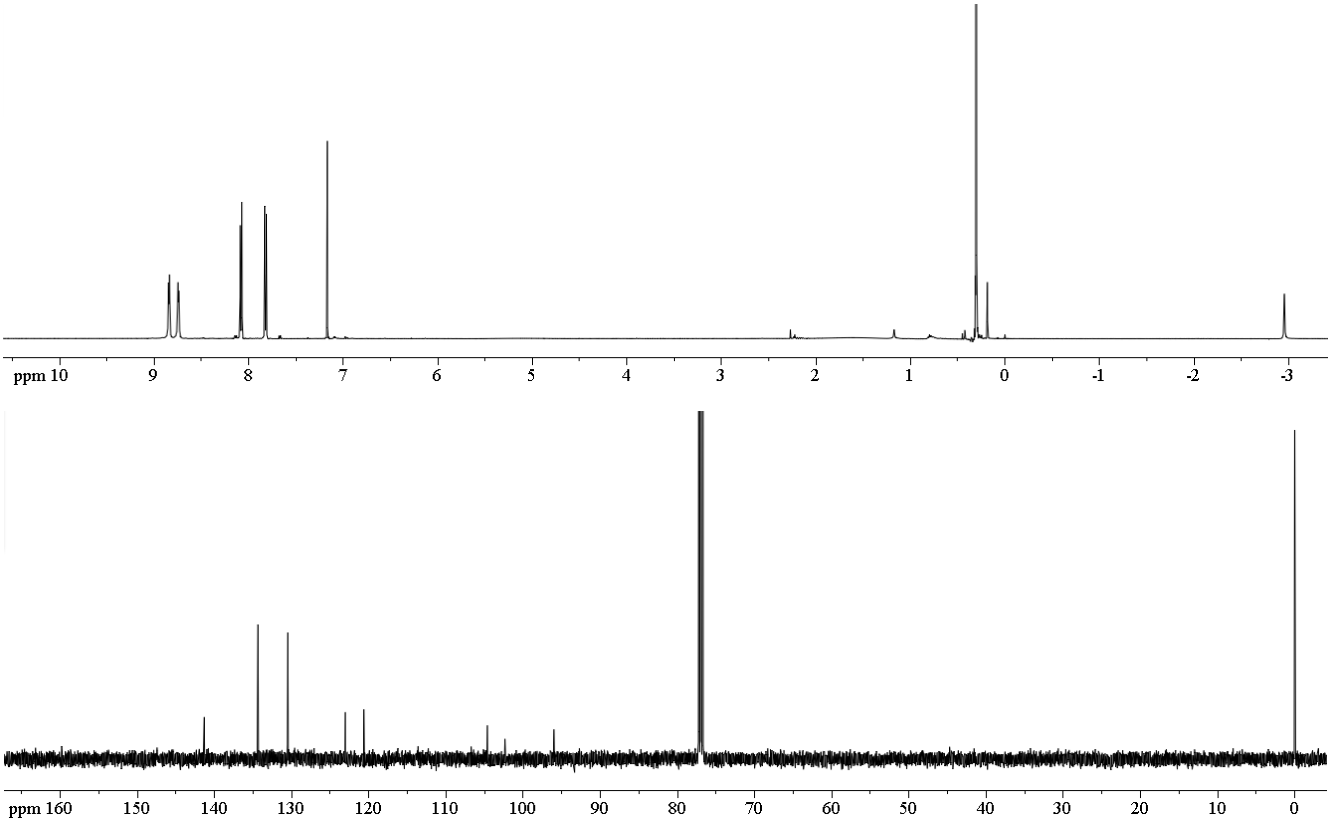

Figure S1. The ^{1}H (top) and ^{13}C (bottom) NMR spectra for 5,15-*bis*(pentafluorophenyl)-10,20-*bis*[4-[2-(trimethylsilyl)ethynyl]phenyl]porphyrin.

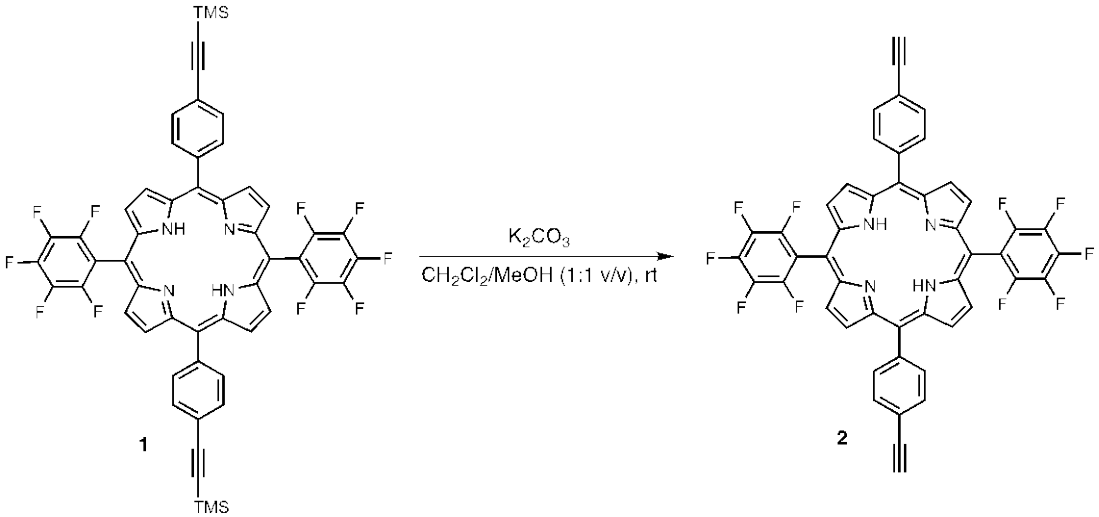

5,15-*Bis*(pentafluorophenyl)-10,20-*bis*(4-ethynylphenyl)porphyrin. Into a 250 mL round-bottom flask equipped with a magnetic stir bar were combined compound **1** (1.0 g, 1.0 mmol), K_2CO_3 (2.8 g, 20 mmol), and CH_2Cl_2/MeOH (100 mL, 1:1 v/v) and the resulting suspension was allowed to stir overnight at room temperature. After filtering off the excess K_2CO_3, the remaining solution was concentrated to dryness under reduced pressure. The crude solid was redissolved in CH_2Cl_2

(150 mL) and the resulting solution was washed with water (3 × 100 mL), dried over Na_2SO_4, filtered, and concentrated to dryness under reduced pressure to yield **2** as a purple solid (835 mg, 1.0 mmol, 98% yield). ^{1}H NMR (499.4 MHz, $CDCl_3$): δ -2.85 (s, 2H, N*H*), 3.35 (s, 2H, CC*H*), 7.93 (d, *J* = 7.5 Hz, 4H, Ar-*H*), 8.19 (d, *J* = 7.5 Hz, 4H, Ar-*H*), 8.84 (d, *J* = 3.5 Hz, 4H, β-*H*), 8.95 (d, *J* = 3.5 Hz, 4H, β-*H*). {^{1}H}^{13}C NMR (125.8 MHz, $CDCl_3$): δ 78.8, 83.5, 102.6, 116.4, 120.7. 122.3, 130.9, 134.6, 141.9, 145.7, 147.7. MALDI-ToF MS (reflective positive mode): Calcd for $C_{48}H_{20}F_{10}N_4$: 842.68, found: *m/z* 841.61 $[M]^+$. UV-vis: (nm, ($\varepsilon \times 10^4$ /$M^{-1}cm^{-1}$)) 416 (45.3), 513 (1.4), 545 (0.3), 588 (0.5), 643 (0.2). See Figure S2 for the NMR spectra.

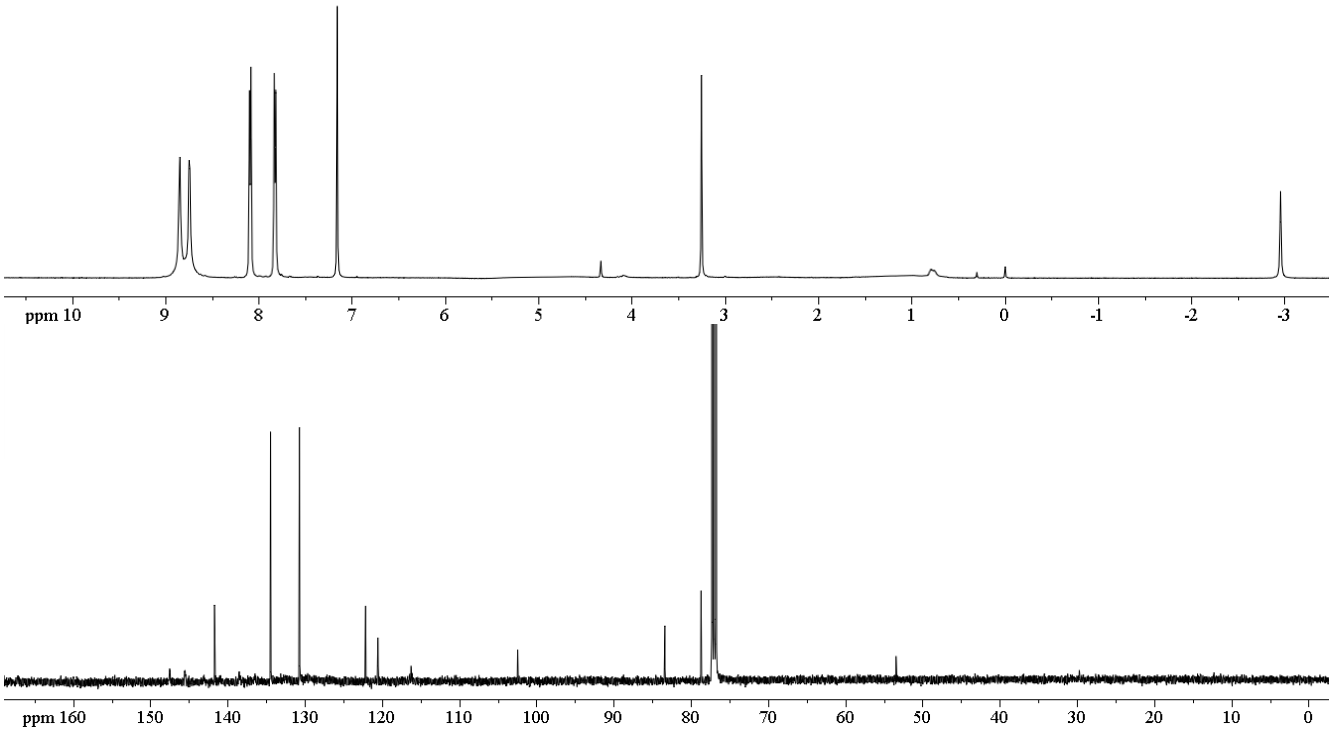

Figure S2. The ^{1}H (top) and ^{13}C (bottom) NMR spectra for 5,15-*bis*(pentafluorophenyl)-10,20-*bis*(4-ethynylphenyl)porphyrin.

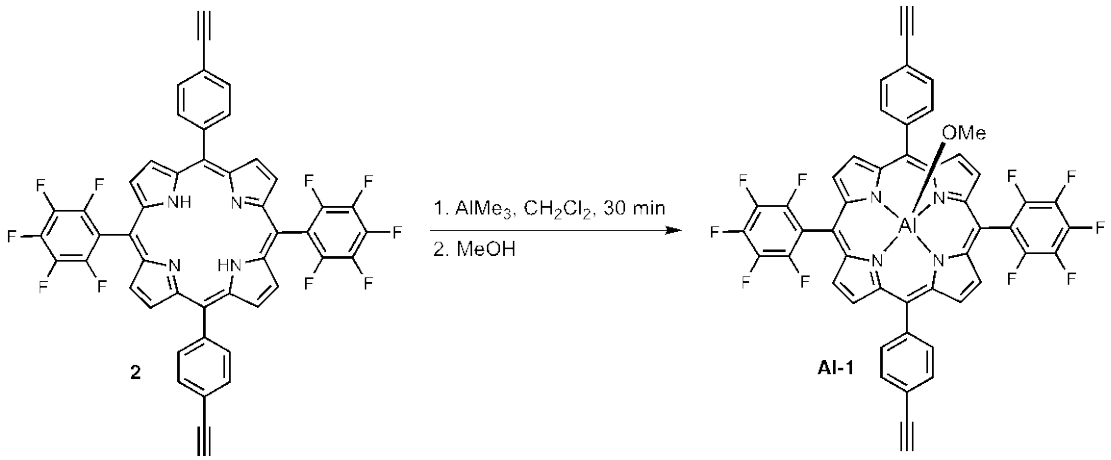

[5,15-*Bis*(pentafluorophenyl)-10,20-*bis*(4-ethynylphenyl)porphyrinato]aluminum(III)methoxide. Into a 100 mL Schlenk flask equipped with a magnetic stir bar were combined compound **2** (250 mg, 0.3 mmol) and anhydrous CH_2Cl_2 (30 mL). At room temperature, a solution of $AlMe_3$ (0.5 mL, 0.9 mmol, 2 M in heptane) was then added using a gas-tight syringe. After stirring for 30 min under N_2, MeOH (10 mL) was added to quench the reaction and the mixture was evaporated to dryness under reduced pressure. The residue was subjected to basic alumina column chromatography (column dimensions = 20 mm × 200 mm, eluent = 5 % MeOH in CH_2Cl_2) to afford compound **3** as a red solid (245 mg, 0.3 mmol, 92 % yield). ^{1}H NMR (499.4 MHz, $CDCl_3$ + 3 drops of MeOD): δ 3.35 (s, 2H, CC*H*), 7.87 (d, *J* = 7.5 Hz, 4H, Ar-

H), 8.10 (d, *J* = 7.5 Hz, 4H, Ar-*H*), 8.95 (d, *J* = 4.5 Hz, 4H, β-*H*), 9.06 (d, *J* = 4.5 Hz, 4H, β-*H*). $\{^1H\}^{13}C$ NMR (125.8 MHz, $CDCl_3$): δ 29.7, 78.9, 83.2, 102.8, 121.1, 122.4, 130.6, 130.7, 133.6, 134.2, 141.2, 146.9, 148.1. MALDI-ToF MS (reflective positive mode): Calcd for $C_{49}H_{21}F_{10}N_4OAl$: 898.68, found: *m/z* 866.48 $[M\text{-}OMe]^+$. UV-vis: (nm, ($\varepsilon \times 10^4$ /$M^{-1}cm^{-1}$)) 420 (41.5), 509 (0.3), 555 (1.2), 594 (0.5). See Figure S3 for the NMR spectra.

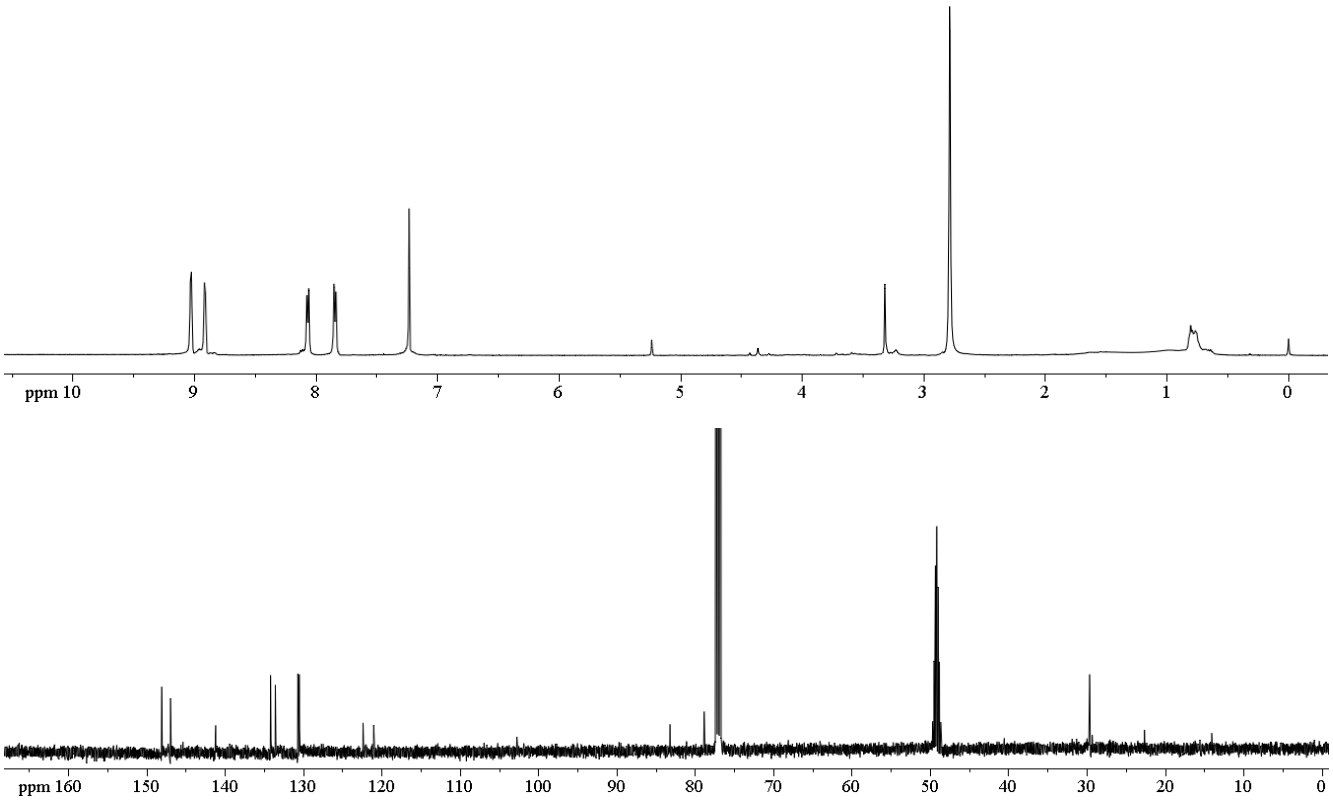

Figure S3. The ^1H (top) and ^{13}C (bottom) NMR spectra for [5,15-*bis*(pentafluorophenyl)-10,20-*bis*(4-ethynylphenyl)porphyrinato]aluminum(III)methoxide.

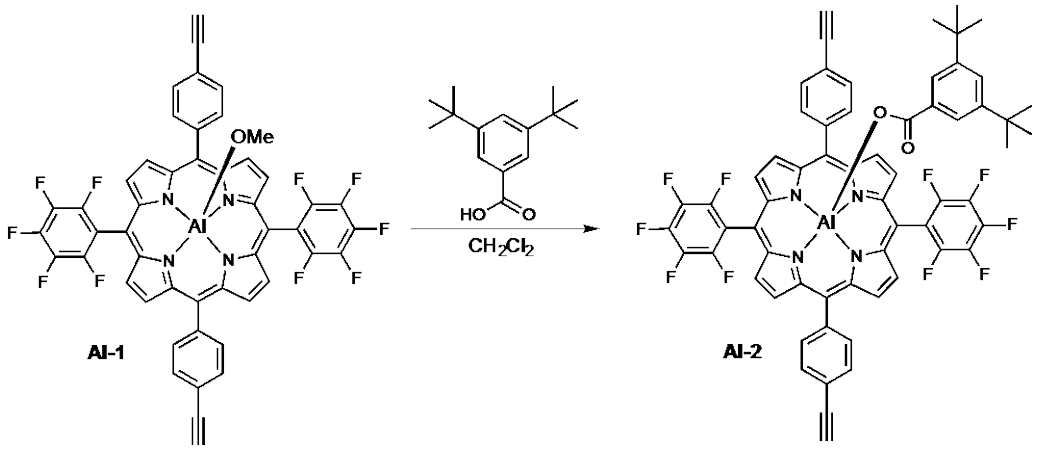

[5,15-*Bis*(pentafluorophenyl)-10,20-*bis*(4-ethynylphenyl)porphyrinato]aluminum(III)(3,5-di-*tert*-butylbenzoate). Compound **3** (100 mg, 0.1 mmol) and 3,5-di-*tert*-butylbenzoic acid (40 mg, 0.2 mmol) were combined with CH_2Cl_2 (30 mL) in a 100 mL round-bottom flask equipped with a magnetic stir bar. The resulting mixture was allowed to stir under N_2 for 12 h at room temperature before being evaporated to dryness using a rotary evaporator. The remaining crude product was redissolved in a minimal amount of CH_2Cl_2 (3 mL) and the product was precipitated out of solution with hexanes (100 mL). Pure product was isolated by filtration as a purple solid (105 mg, 0.09 mmol, 87 % yield). ^1H NMR (499.4 MHz, $CDCl_3$): δ 0.68 (s, 18H, $C(CH_3)_3$), 3.34 (s, 2H, C*CH*), 4.93 (s, 2H, Ar-*H*), 6.72 (s, 1H, Ar-*H*), 7.69 (s, 4H, Ar-*H*), 7.93 (s, 4H, Ar-*H*), 9.04 (d, *J* = 4.5 Hz, 4H, β-*H*), 9.17 (d, *J* = 4.5 Hz, 4H, β-*H*). $\{^1H\}^{13}C$ NMR (125.8 MHz, $CDCl_3$): δ 29.9, 30.9, 31.5, 34.1, 35.1, 78.8, 83.5, 103.4, 121.3, 121.8, 122.4, 124.5, 128.1, 130.8, 133.9, 141.4, 147.9, 148.8, 149.1, 151.3, 162.9,

172.2. MALDI-ToF MS (reflective positive mode): Calcd for $C_{63}H_{39}F_{10}N_4O_2Al$: 1100.97, found: *m/z* 1100.89 $[M]^+$, 867.09 [M-3,5-di-*tert*-butyl benzoate]$^+$. UV-vis: (nm, ($\varepsilon \times 10^4$ /$M^{-1}cm^{-1}$)) 420 (43.5), 510 (0.3), 556 (1.2), 594 (0.5). See Figure S4 for the NMR spectra.

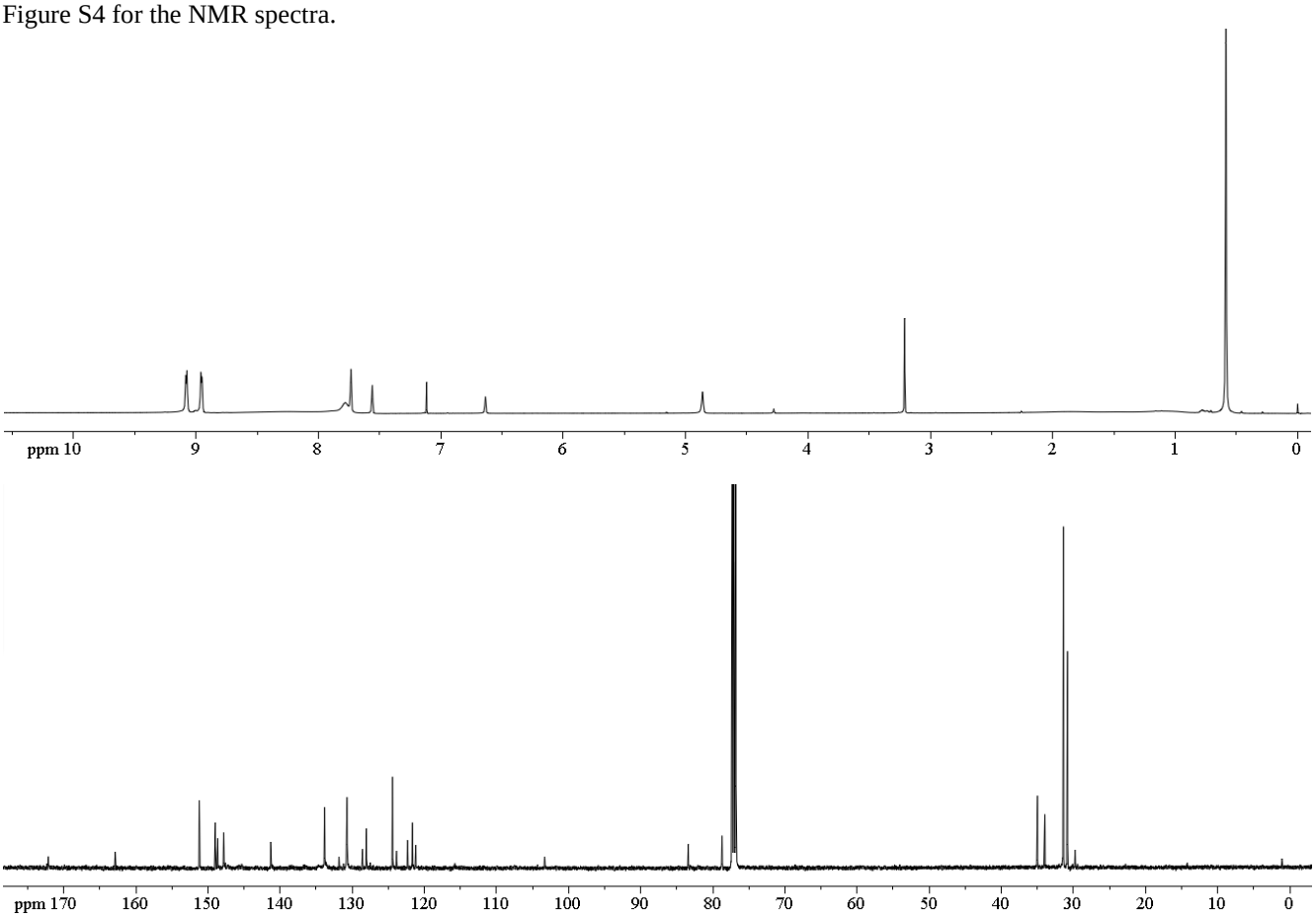

Figure S4. The ^1H (top) and ^{13}C (bottom) NMR spectra for [5,15-*bis*(pentafluorophenyl)-10,20-*bis*(4-ethynylphenyl)porphyrinato]aluminum(III)(3,5-di-*tert*-butylbenzoate).

S4. Preparation of Al-PPOPs by thermal activation.

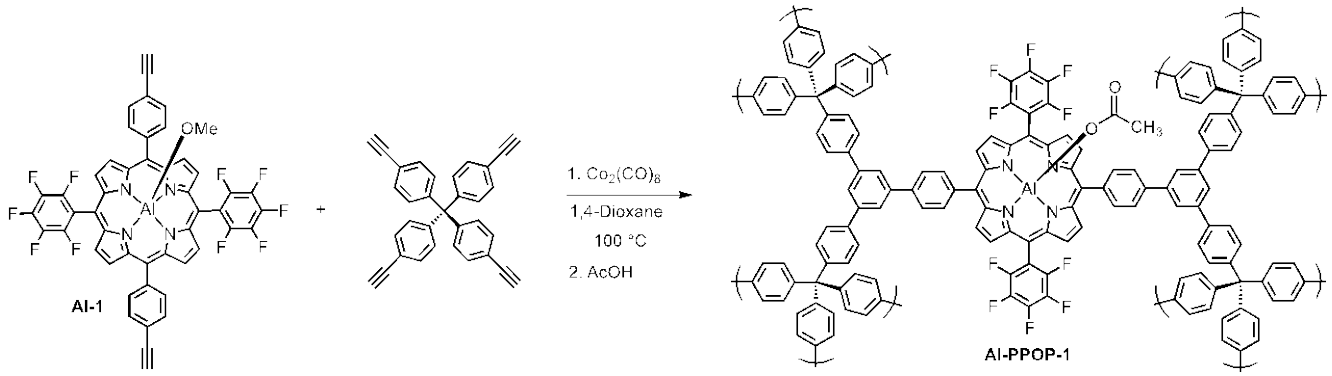

Al-PPOP-1. In a nitrogen glovebox, a 20 mL microwave vial (capacity designates the amount of solution that can be safely loaded) equipped with a magnetic stir bar was charged with **Al-1** (100 mg, 0.1 mmol), *tetrakis*(4-ethynylphenyl)methane (23 mg, 0.5 mmol), and dry 1,4-dioxane (14 mL). $Co_2(CO)_8$ (19 mg, 0.05 mmol) was then added to the resulting solution and the microwave vial was sealed with a crimp cap. The vial was removed from the glovebox and placed into a 100 ºC oil bath where the reaction mixture was allowed to stir for 1.5 h. The solution thickened and precipitates were observed after about 5 min; after 10 min, significant gelation could be observed. After 1.5 h, the vial was removed from the oil bath and cooled down slightly; the crimp cap was removed and acetic acid (1 mL) was then added to the mixture. A spatula was used to broken up the gel into smaller particles; the vial was crimp-capped again, put back into

the 100 ºC oil bath, and kept there while stirring for 1 h. The hot reaction mixture was then filtered through a fine-fritted glass funnel and the remaining purple solid was washed with THF (30 mL), MeOH (30 mL), and H_2O (30 mL). Removal of solvent under vacuum at 150 ºC gave a purple solid (118 mg, 96 % yield). Anal.: Calcd for $(C_{133}H_{62}F_{20}N_8O_4Al_2)_n$: C, 70.37; H, 2.75; N, 4.94. Found: C, 62.91; H, 3.19; N, 4.07. ICP-OES: Calcd for $(C_{133}H_{62}F_{20}N_8O_4Al_2)_n$: 2.4 wt% Al. Found: 2.1 wt% Al. See Figure S5 for the solid-state ^1H-^{13}C CP-MAS NMR spectrum.

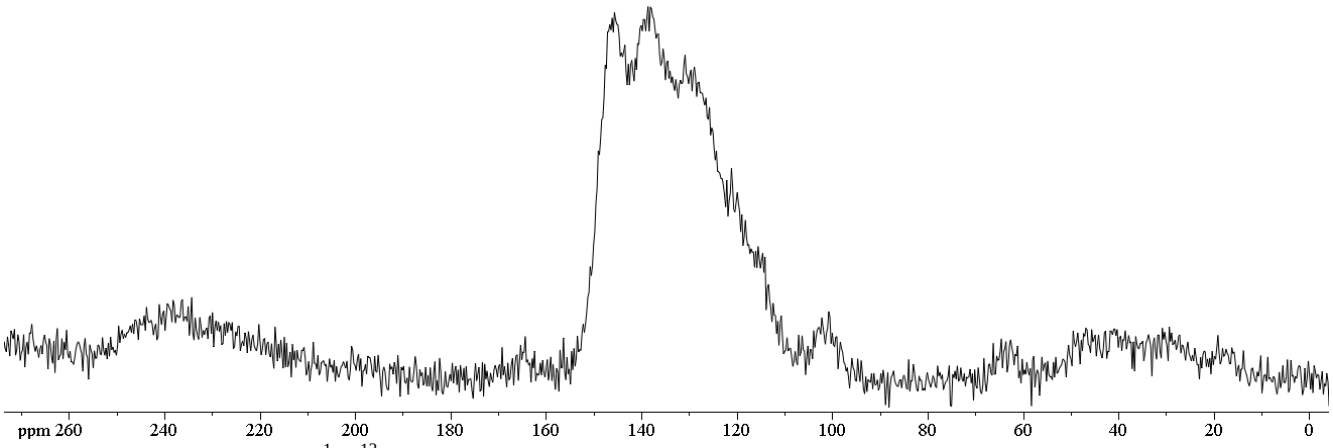

Figure S5. The solid-state ^1H-^{13}C CP-MAS NMR spectrum of **Al-PPOP-1** recorded at a MAS rate of 10 kHz.

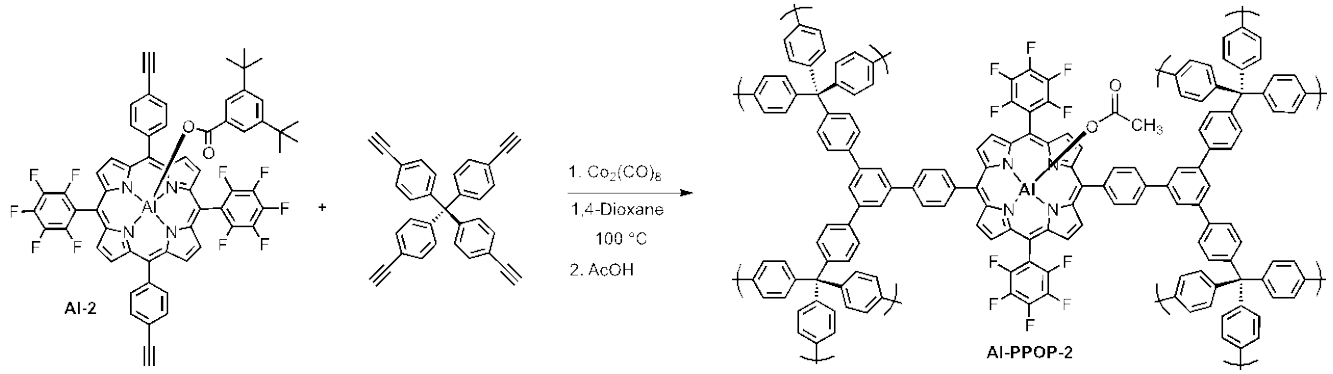

Al-PPOP-2. **Al-PPOP-2** was synthesized under the same protocol and scale as described for **Al-PPOP-1**, with exception to the amount of **Al-2**: (122 mg, 0.1 mmol). Product was isolated as a purple solid (120 mg, 98 % yield). Anal.: Calcd for $(C_{133}H_{62}F_{20}N_8O_4Al_2)_n$: C, 70.37; H, 2.75; N, 4.94. Found: C, 66.11; H, 2.96; N, 4.54. ICP-OES: Calcd for $(C_{133}H_{62}F_{20}N_8O_4Al_2)_n$: 2.4 wt% Al. Found: 2.1 wt% Al. See Figure S6 for the solid-state ^1H-^{13}C CP-MAS NMR spectrum.

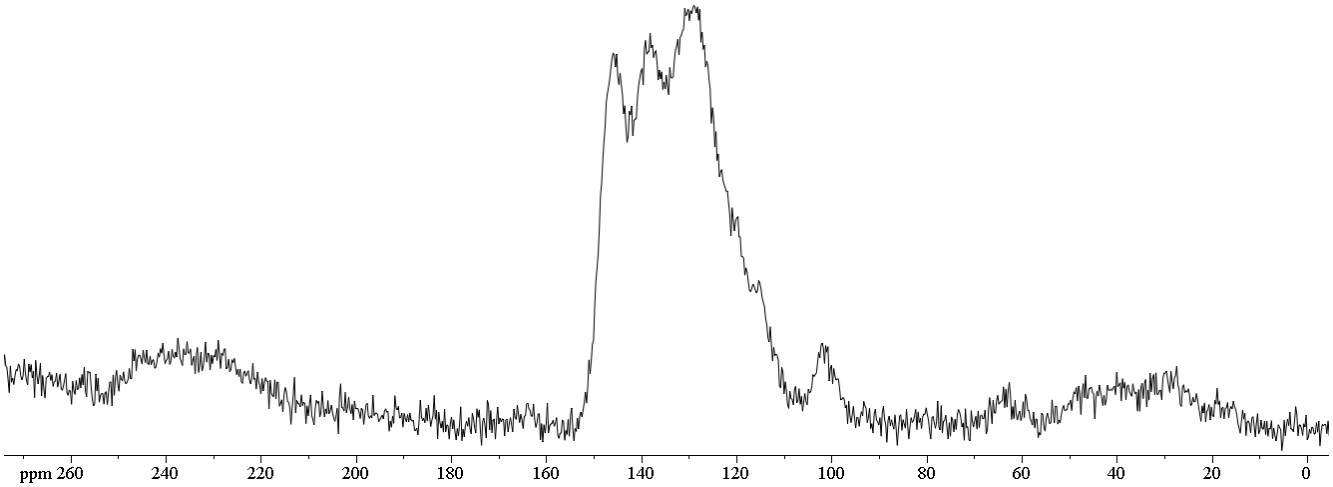

Figure S6. The solid-state ^1H-^{13}C CP-MAS NMR spectrum of **Al-PPOP-2** recorded at a MAS rate of 10 kHz.

S5. Preparation of Al-PPOPs by supercritical CO_2 processing.

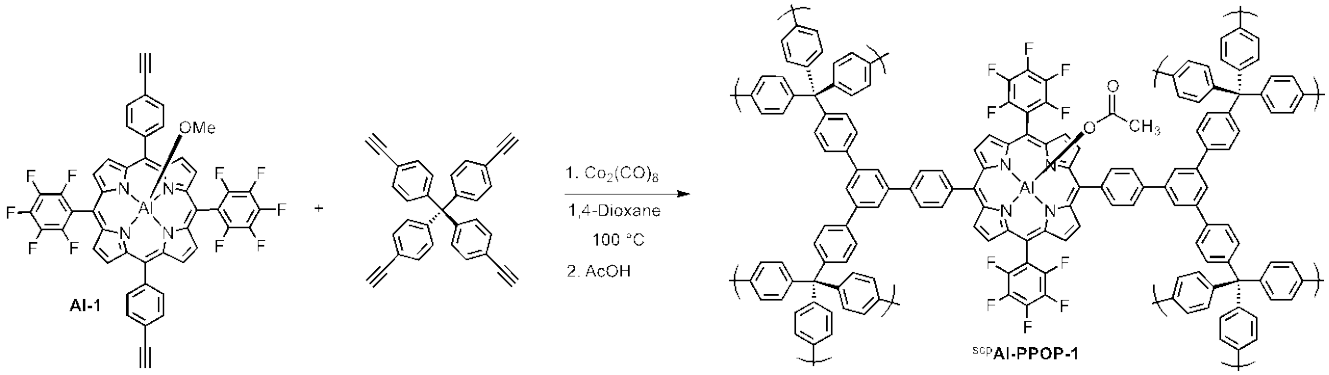

[scp]**Al-PPOP-1**. **Al-PPOP-1** was synthesized under the same protocol and scale as described in section S4 but was worked up differently after the acetic acid-quenching step. At this point, the hot reaction mixture was filtered over a fine-fritted glass funnel and the remaining purple solid was rinsed thoroughly with absolute ethanol (~100 mL), taking care to continually keep a layer of ethanol over the solid (it is critical to never allow the polymer sample to dry in air as it will irreversibly shrink). The remaining fine slush was transferred into an 8 dram vial by pipette, using ethanol to complete transfer, bringing the total volume to 20 mL. This suspension was allowed to stir overnight at room temperature before being poured into a fine-fritted glass filter; the remained purple solid was rinsed thoroughly with ethanol (~50 mL), again with care being taken to continually keep a layer of ethanol over the solid.

The remaining fine slush was again transferred into a 20 mL scintillation vial by pipette, using ethanol to complete transfer; however, the total volume was kept to about 2 mL. The vial was then placed inside a Tousimis™ Samdri® PVT-30 critical point dryer (Tousimis, Rockville, MD) that has been retrofitted to fit the 20 mL vial. The ethanol was then exchanged with liquid CO_2 (maintained at ~ 0-10 ^oC) over a period of 8 h. Every hour, the liquid CO_2 and ethanol mixture were vented under positive pressure for 2 minutes (most of the liquid has been evaporated after 30 s), taking care to maintain the rate of venting below the rate of filling so that the drying chamber remains full. After 8 h, the temperature inside the sealed chamber was raised to 38 ºC, which increased the pressure to above the critical point of CO_2 at 1300 psi. This pressure was maintained for 30 minutes; then the chamber was slowly vented over a period of 12 h while being kept at 38 ºC. Nitrogen adsorption was carried out immediately on the dried sample. Anal.: Calcd for $(C_{133}H_{62}F_{20}N_8O_4Al_2)_n$: C, 70.37; H, 2.75; N, 4.94. Found: C, 65.16; H, 2.95; N, 4.48.

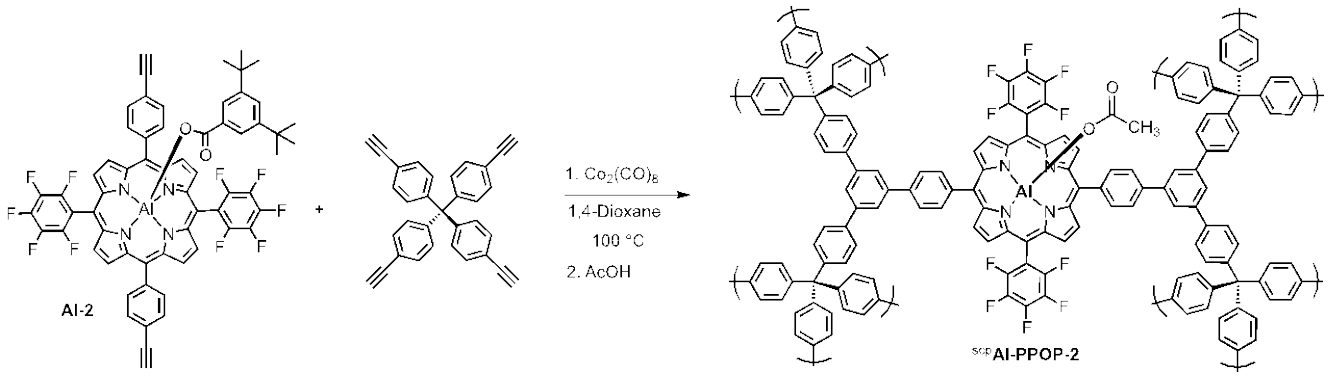

[scp]**Al-PPOP-2**. **Al-PPOP-2** was synthesized under the same protocol and scale as described in section S4 and processed via supercritical CO_2 as detailed for [scp]**Al-PPOP-1**. Anal.: Calcd for $(C_{133}H_{62}F_{20}N_8O_4Al_2)_n$: C, 70.37; H, 2.75; N, 4.94. Found: C, 65.05; H, 3.01; N, 4.38.

S6. Product formation rates for the methanolysis of PNPDPP by Al-PPOPs. Reactions were carried out with Al-PPOP catalysts and conversion data was collected by UV-vis spectroscopy. As an example, the determination of the product formation rate for [scp]**Al-PPOP-2** was carried out as follows. On the bench-top, a 5 mL microwave vial was charged with PNPDPP (37 mg, 25 mM), [scp]**Al-PPOP-2** (5.4 mg, 4 mol% Al^{III}), and methanol (4 mL). The reaction vial was sealed with a crimp cap and allowed to stir 60 °C in an oil bath. Periodically, the reaction vial was removed from the oil bath, cooled down to below 50 °C with a quick spray of hexanes (~5 s) to prevent excessive MeOH evaporation, and quickly opened for aliquot (100 μL) sampling before being crimp-capped again and placed back in the oil bath. The sampled aliquot was diluted with MeOH to 25 mL in a volumetric flask and analyzed by UV-vis spectroscopy. The conversion of PNPDPP as a

function of reaction time was obtained by monitoring the increase of absorbance of *p*-nitrophenol at 311 nm (see Figures S7-S8 and Table S1).

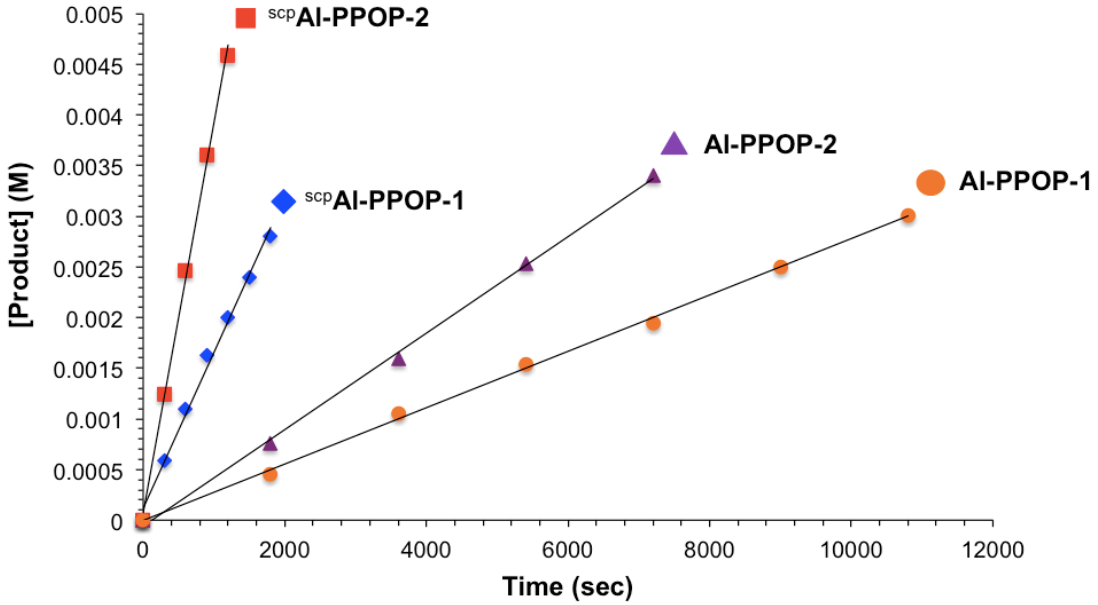

Figure S7. Initial product formation rates for the methanolysis of PNPDPP in the presence of Al-PPOP catalysts: ^{scp}**Al-PPOP-2**, red squares; ^{scp}**Al-PPOP-1**, blue diamonds; **Al-PPOP-2**, purple triangles; **Al-PPOP-1**, orange circles.

Table S1. Product formation rates for the methanolysis of PNPDPP in the presence and absence of Al-PPOP catalysts.

Al-PPOP catalyst	Catalyst loading (mol%)	Observed initial rate (M/s)	Relative rate *vs.* uncat. reaction	Al^{III} leaching (% of Al^{III} loading)
Al-PPOP-1	4	2.8×10^{-7}	17	0
Al-PPOP-2	4	4.8×10^{-7}	28	0
^{scp}**Al-PPOP-1**	4	1.5×10^{-6}	88	0
^{scp}**Al-PPOP-2**	4	3.5×10^{-6}	205	0
Uncatalyzed	0	1.7×10^{-8}	0	0

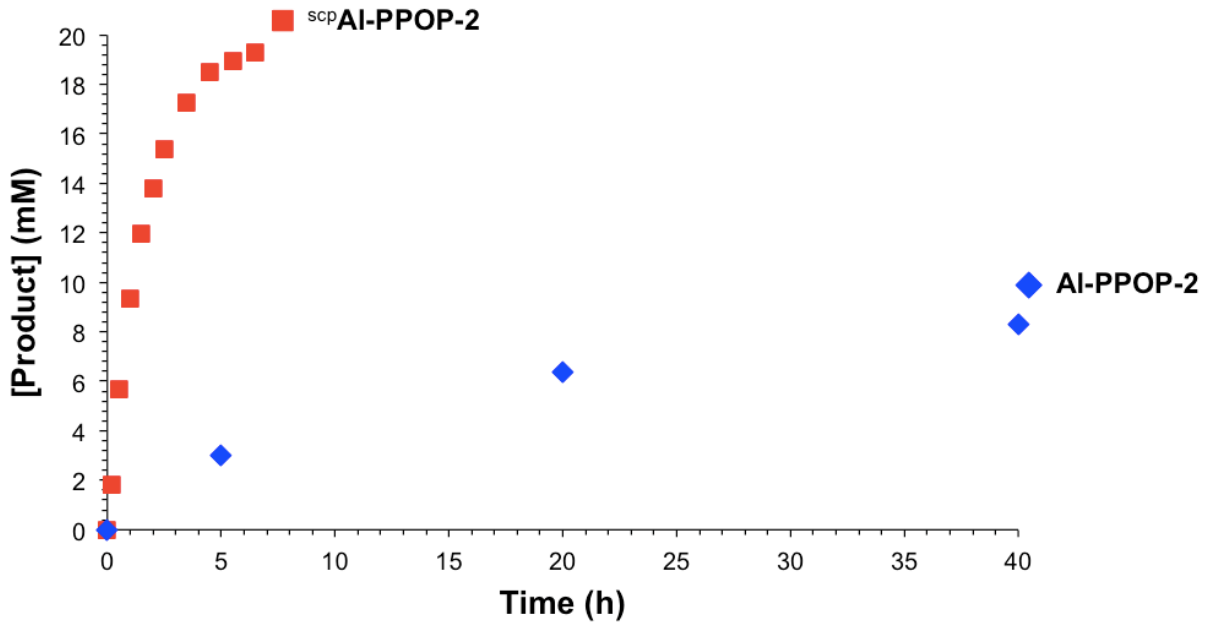

Figure S8. Overall product formation profiles for the methanolysis of PNPDPP in the presence of Al-PPOP catalysts. ^{scp}**Al-PPOP-2**, red squares; **Al-PPOP-2**, blue diamonds.

S7. Initial product formation rate for the methanolysis of PNPDPP in the presence of finely-ground Al-PPOP-2. Using a mortar and pestle, **Al-PPOP-2** was ground into a fine powder and its initial methanolysis rate was determined as described in section S6.

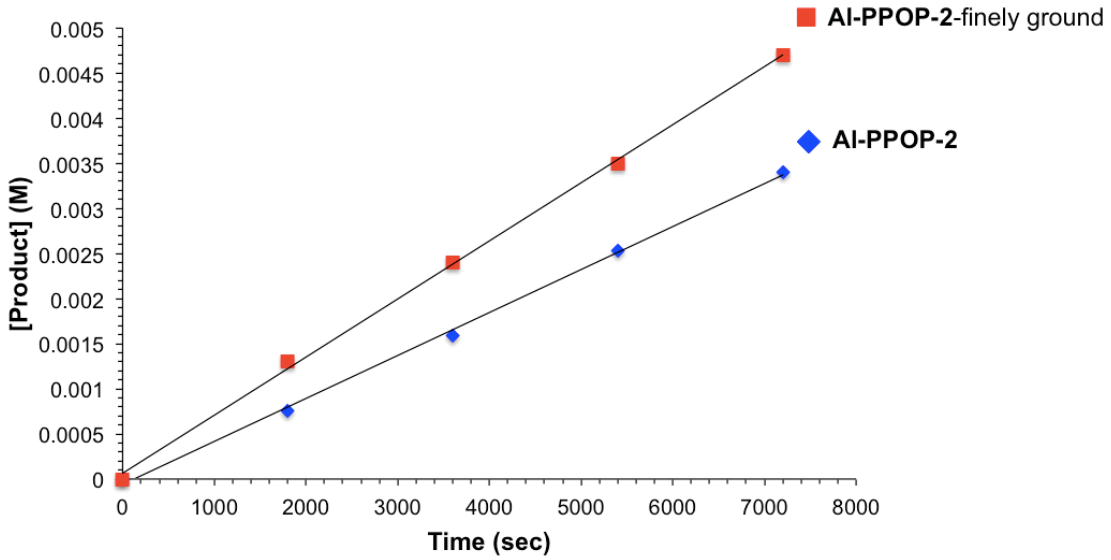

Figure S9. Initial product formation rates for the methanolysis of PNPDPP in the presence of Al-PPOP catalysts: **Al-PPOP-2**-finely ground, red squares; **Al-PPOP-2**, blue diamonds.

Table S2. Product formation rates for the methanolysis of PNPDPP in the presence of Al-PPOP catalysts.

Al-PPOP catalyst	Catalyst loading (mol%)	Observed initial rate (M/s)	Relative rate *vs.* uncat. reaction
Al-PPOP-2	4	4.8×10^{-7}	28
Al-PPOP-2-finely ground	4	6.4×10^{-7}	38

S8. Second methanolysis cycle of ^{scp}Al-PPOP-2.

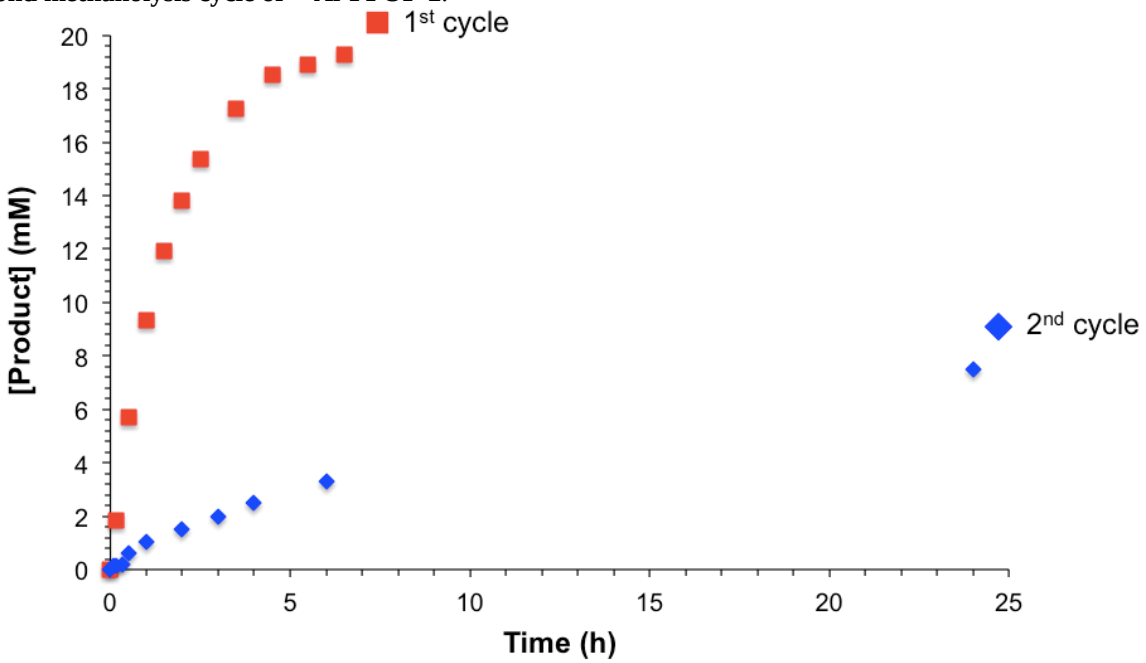

Figure S10. Overall product formation profiles for the methanolysis of PNPDPP in the presence of ^{scp}**Al-PPOP-2**. First cycle, red squares; second cycle, blue diamonds.

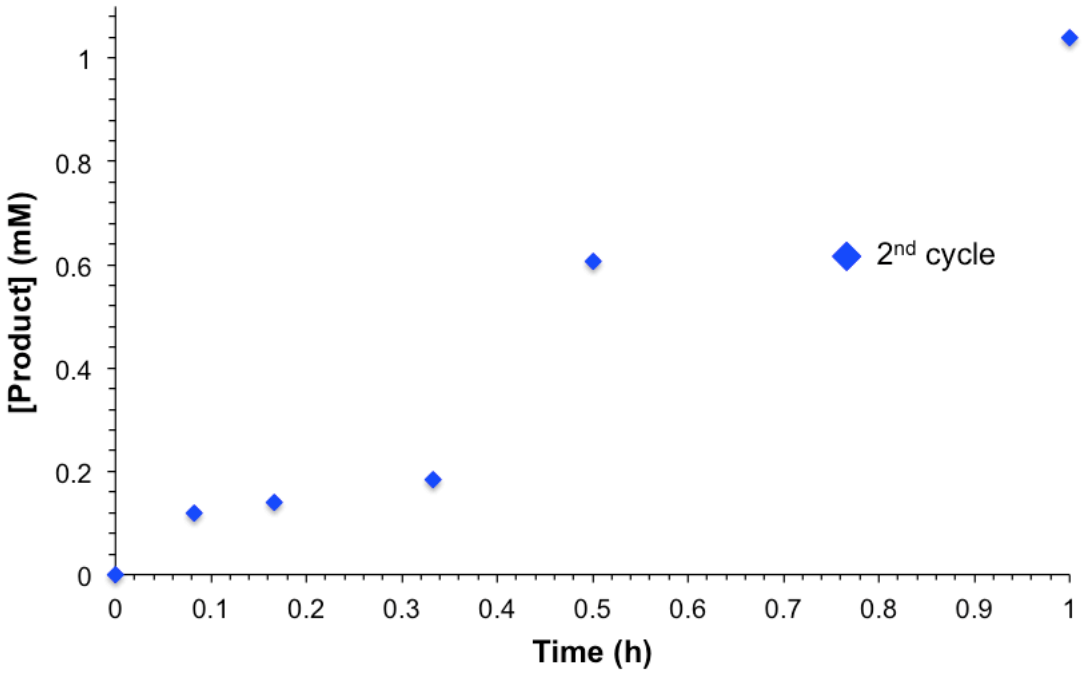

Figure S11. First hour of the second cycle for the methanolysis of PNPDPP in the presence of ^{scp}**Al-PPOP-2** showing a 30-minute induction period.

S9. Soxhlet extraction after each PNPDPP methanolysis cycle for ^{scp}Al-PPOP-2. After each PNPDPP methanolysis cycle, ^{scp}**Al-PPOP-2** (5.4 mg initial mass) was transferred to a glass thimble and Soxhlet-extracted with MeOH for 24 hours. The UV-vis spectrum of the resulting filtrate revealed the presence of 2.1 mg of *p*-nitrophenol after the first cycle and 1.3 mg of *p*-nitrophenol after the second cycle.

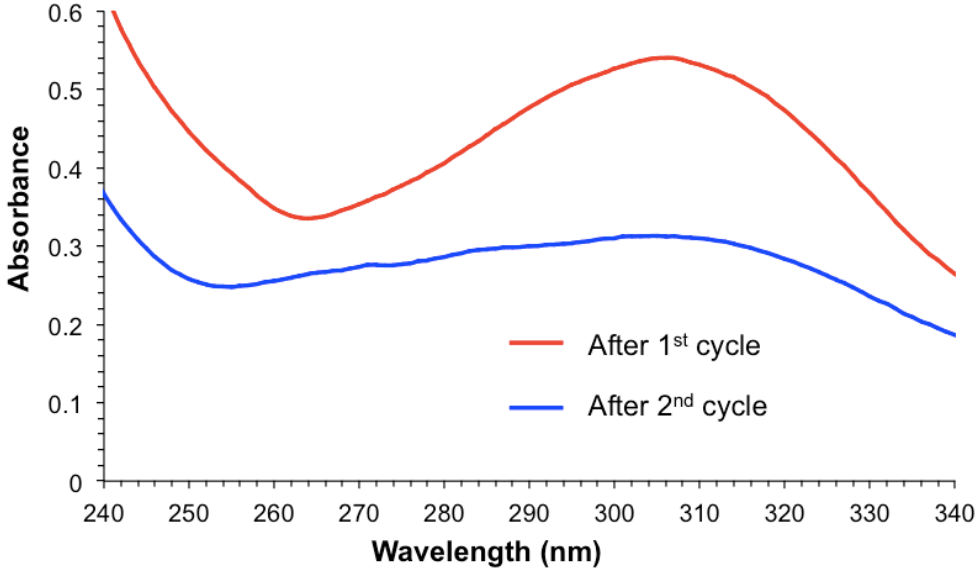

Figure S12. UV-vis spectrum of the filtrate obtained after 24 h of MeOH-based Soxhlet extractions of ^{scp}**Al-PPOP-2** after the first (red line) and second (blue line) PNPDPP methanolysis cycles.

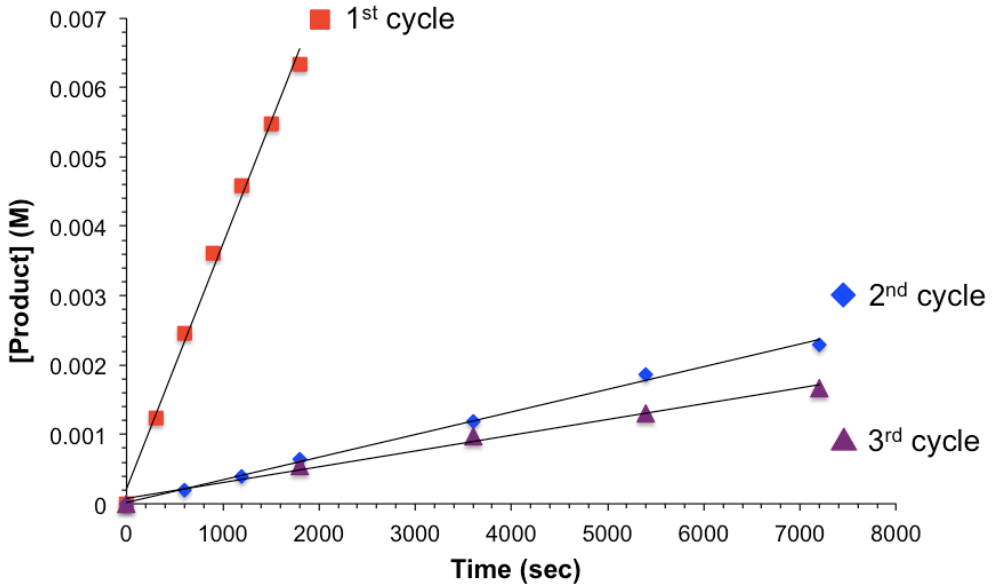

Figure S13. Initial product formation rates for the methanolysis of PNPDPP in the presence of ^{scp}**Al-PPOP-2** after methanol Soxhlet extractions. First cycle, red squares; second cycle, blue diamonds; third cycle, purple triangles.

Table S3. Product formation rates for the methanolysis of PNPDPP in the presence of ^{scp}**Al-PPOP-2** after Soxhlet extractions.

Al-PPOP catalyst	Cycle	Catalyst loading (mol%)	Observed initial rate (M/s)	Relative rate *vs.* uncat. reaction	Al^{III} leaching (% of Al^{III} loading)
^{scp}**Al-PPOP-2**	1	4	3.5×10^{-6}	205	0
	2	4	3.3×10^{-7}	20	0
	3	4	2.3×10^{-7}	14	0

S10. Regeneration of ^{scp}Al-PPOP-2 after the first PNPDPP methanolysis cycle. After the first cycle of methanolysis, ^{scp}**Al-PPOP-2** isolated by filtration through a fine-fritted glass filter and rinsed thoroughly with absolute ethanol. The sample was then reprocessed with supercritical CO_2 as described in section S5. The reactivated sample was then used for the second cycle of PNPDPP methanolysis.

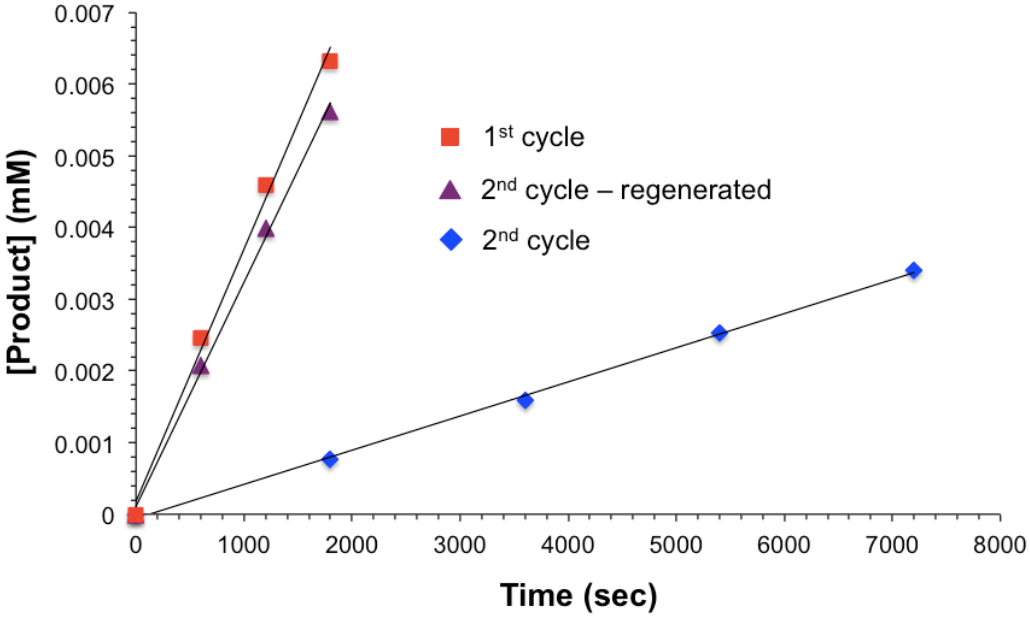

Figure S14. Initial product formation rates for the methanolysis of PNPDPP in the presence of ^{scp}**Al-PPOP-2**. First cycle, red squares; second cycle, blue diamonds; second cycle-regenerated, purple triangles.

Table S4. Product formation rates for the methanolysis of PNPDPP in the presence of ^{scp}**Al-PPOP-2**.

Al-PPOP catalyst	Cycle	Catalyst loading (mol%)	Observed initial rate (M/s)	Relative rate *vs.* uncat. reaction
^{scp}**Al-PPOP-2**	1	4	3.5×10^{-6}	205
	2	4	3.3×10^{-7}	20
	2[a]	4	3.1×10^{-6}	182

[a]After reprocessing with supercritical CO_2.

S11. N_2 isotherms of Al-PPOPs.

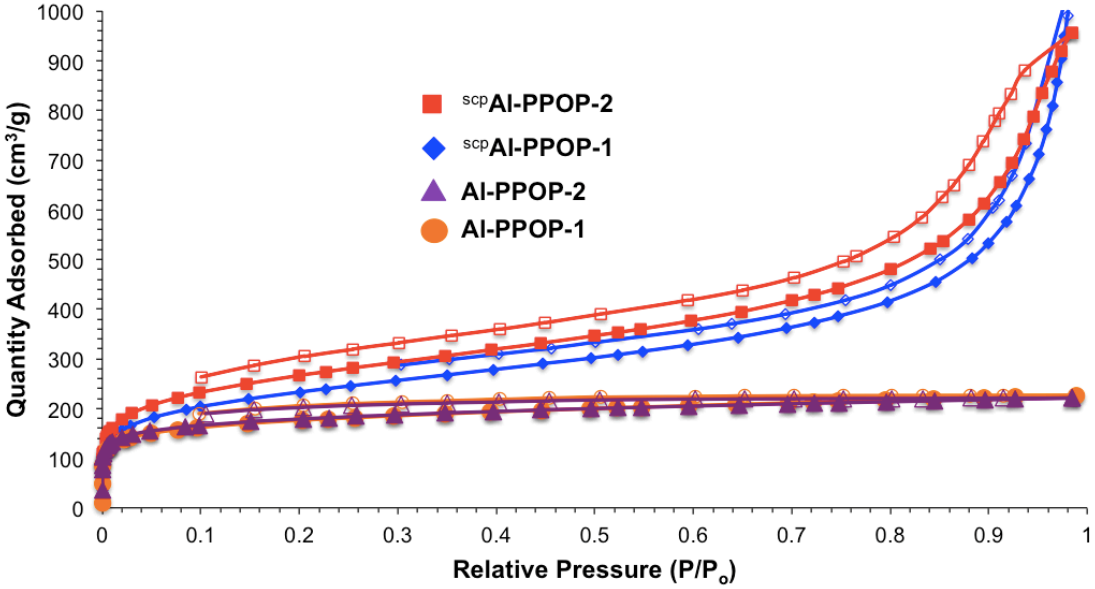

Figure S15. The N_2 isotherms of Al-PPOPs recorded at 77 K. Closed symbols = adsorption; open symbols = desorption.

S12. Pore size distributions of Al-PPOPs.

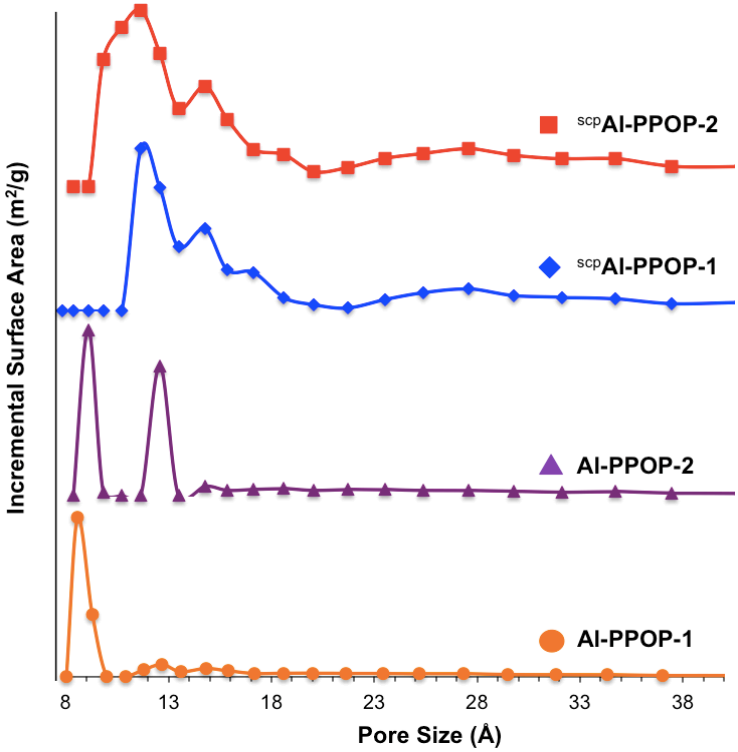

Figure S16. The pore size distribution plots for Al-PPOP derivatives according to DFT analysis of the N_2 adsorption isotherms.

S13. N_2 isotherm of regenerated ^{scp}Al-PPOP-2.

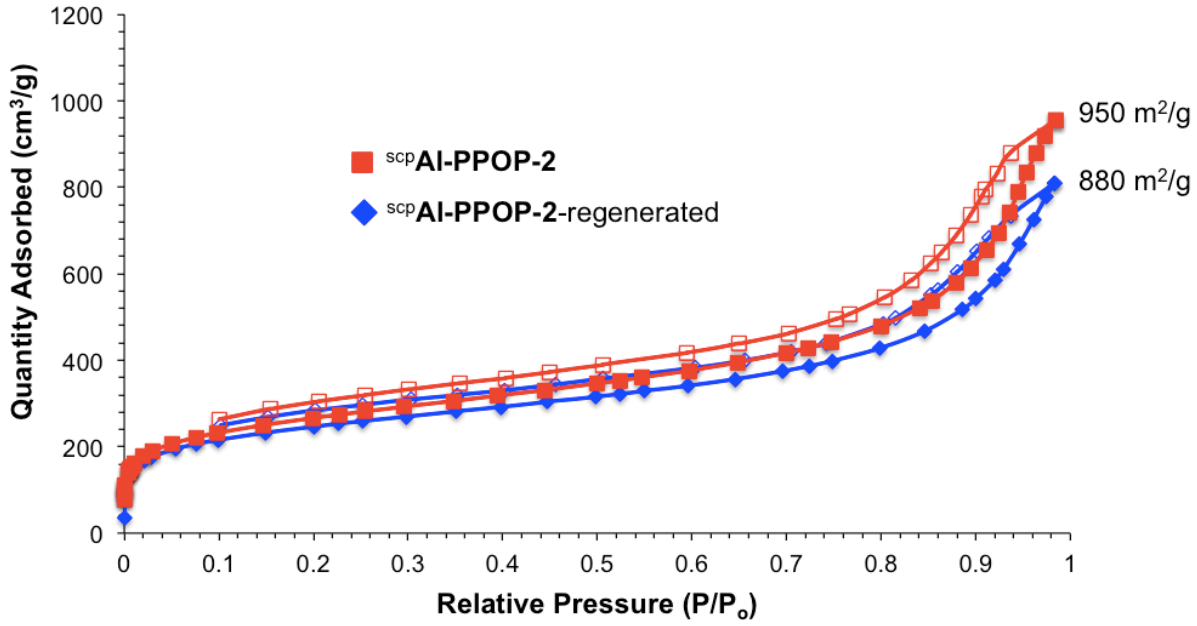

Figure S17. The N_2 isotherms of ^{scp}**Al-PPOP-2** and ^{scp}**Al-PPOP-2**-regenerated recorded at 77 K. Closed symbols = adsorption; open symbols = desorption.

S14. Pore size distribution of regenerated ^{scp}Al-PPOP-2.

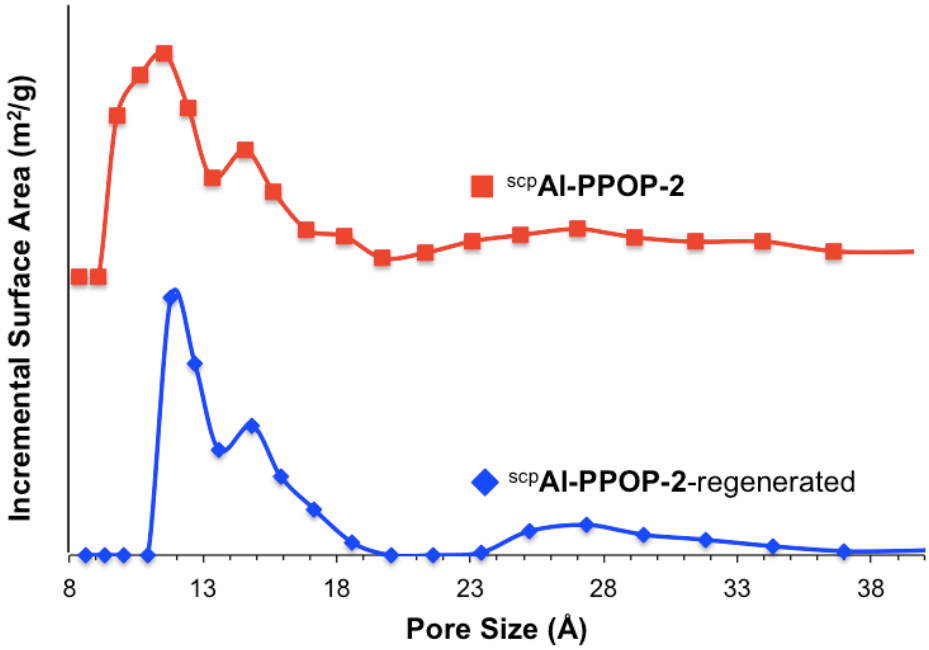

Figure S18. The pore size distribution plots for ^{scp}**Al-PPOP-2** and ^{scp}**Al-PPOP-2**-regenerated according to DFT analysis of the N_2 adsorption isotherms.

S15. Thermal gravimetric analysis data for Al-PPOPs.

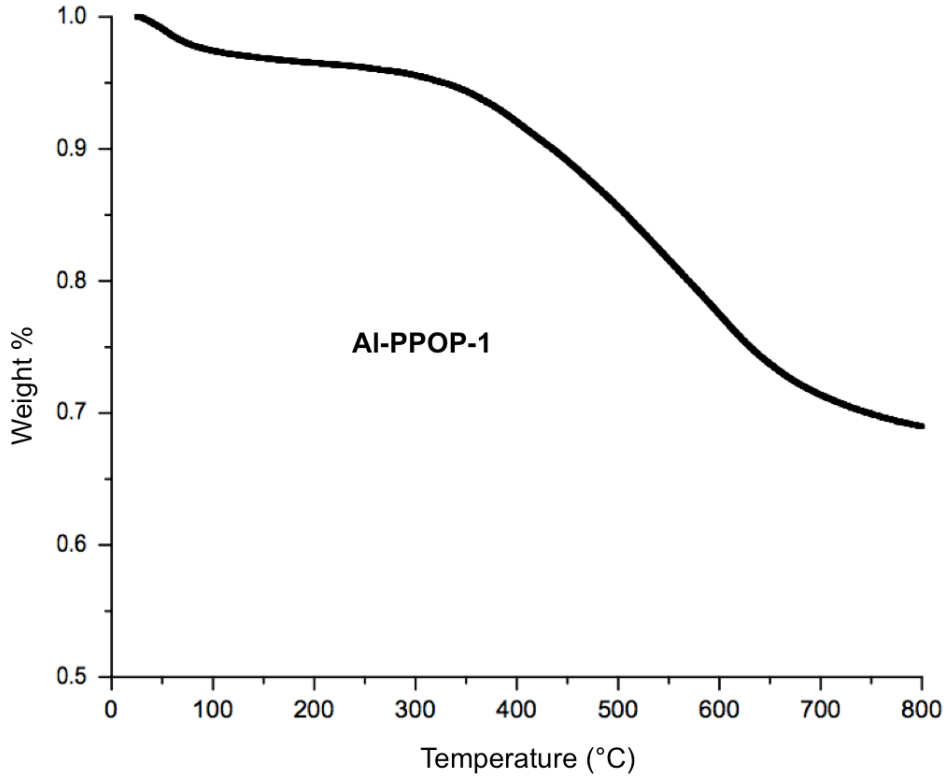

Figure S19. The TGA profile of **Al-PPOP-1** measured under N_2.

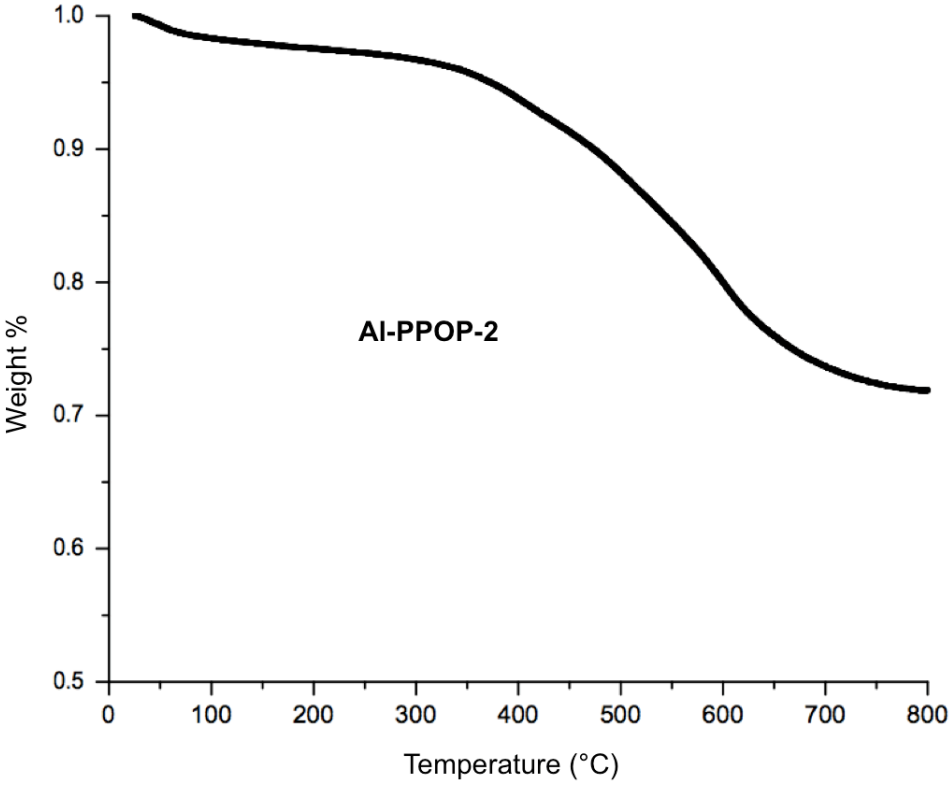

Figure S20. The TGA profile of **Al-PPOP-2** measured under N_2.

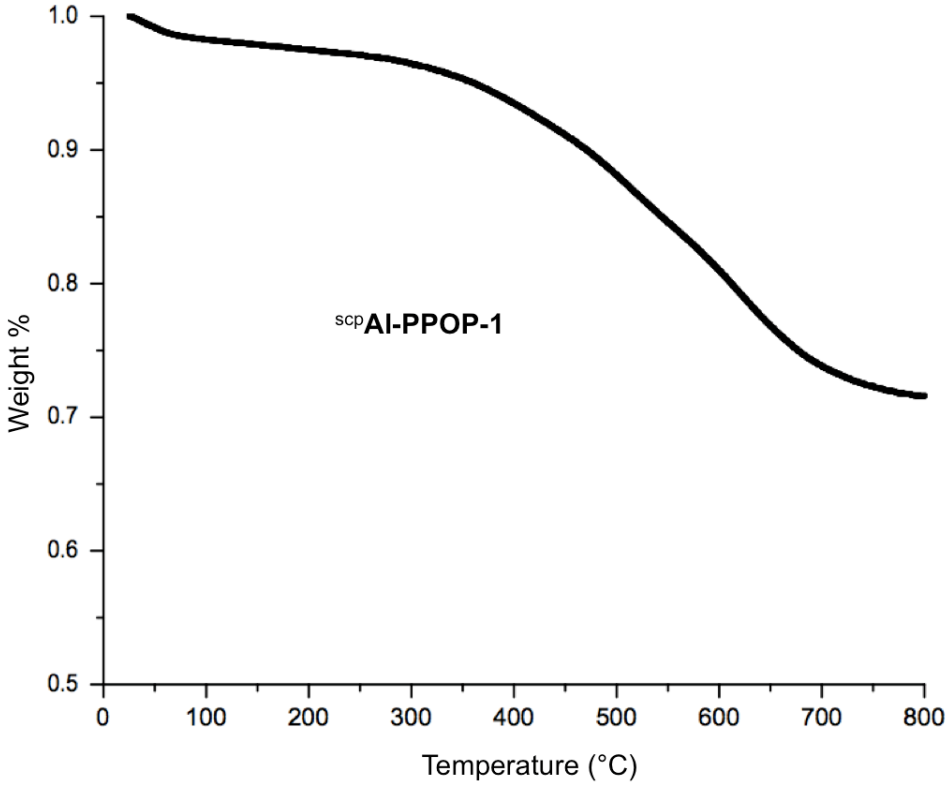

Figure S21. The TGA profile of ^{scp}**Al-PPOP-1** measured under N_2.

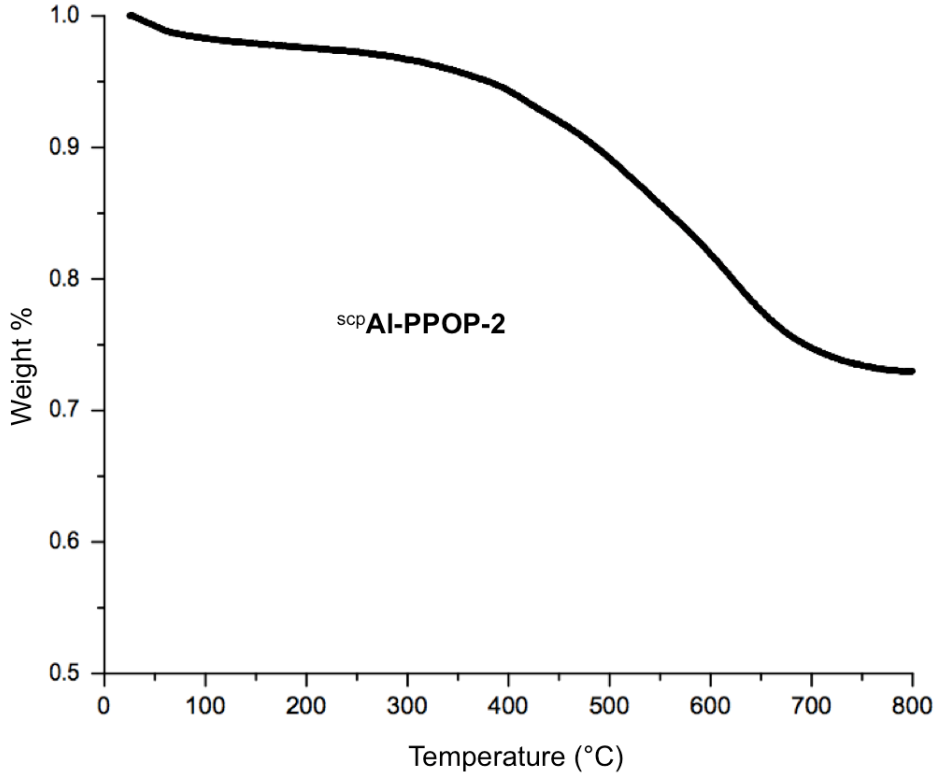

Figure S22. The TGA profile of ^{scp}**Al-PPOP-2** measured under N_2.

S16. Densities of Al-PPOP catalysts. According to Lowell *et al.*,[S6] the *skeletal density* is the ratio of the mass to the volume occupied by the *framework* of the sample excluding the volume of any open pores while the *bulk density* is the ratio of the mass to the volume occupied by the *whole* sample, including all internal pore and interparticle void space (*pore volume*). Hence, the bulk density can be calculated if the measured skeletal density and the total pore volume of each material are known (Eq S1).

$$\rho_{bulk} = 1/[(1/\rho_{skeletal}) + V_{total\ pore}] \quad \text{(S1)}$$

Table S5. Densities of Al-PPOP catalysts.

Al-PPOP catalyst	Total NLDFT-derived pore volume (cm^3/g)[a]	$\rho_{skeletal}$ (g/cm^3)[b]	NLDFT-derived ρ_{bulk} (g/cm^3)[c]
Al-PPOP-1	0.35	1.49	0.98
Al-PPOP-2	0.34	1.48	0.98
^{scp}**Al-PPOP-1**	1.02	1.42	0.58
^{scp}**Al-PPOP-2**	1.15	1.37	0.53

[a]Total NLDFT-derived pore volume from the N_2 adsorption profiles at P/P_o = 0.98. [b]Derived from helium pycnometry. Data is averaged from ten measurements with standard deviations of less than 0.01. [c]The bulk densities calculated using the NLDFT-derived pore volumes.

S17. Methanol vapor isotherms of Al-PPOPs.

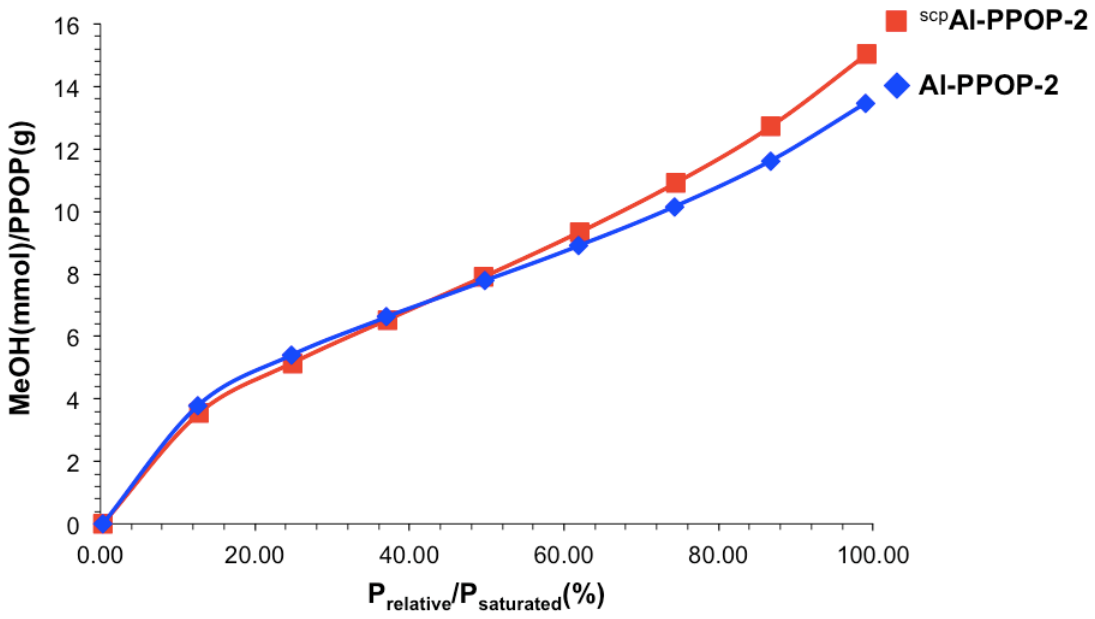

Figure S23. MeOH vapor adsorption isotherm measured at 298 K for ^{scp}**Al-PPOP-2** (red squares) and **Al-PPOP-2** (blue diamonds).

S18. Photographic images of Al-PPOP displaying contrast between conventional and supercritical activation.

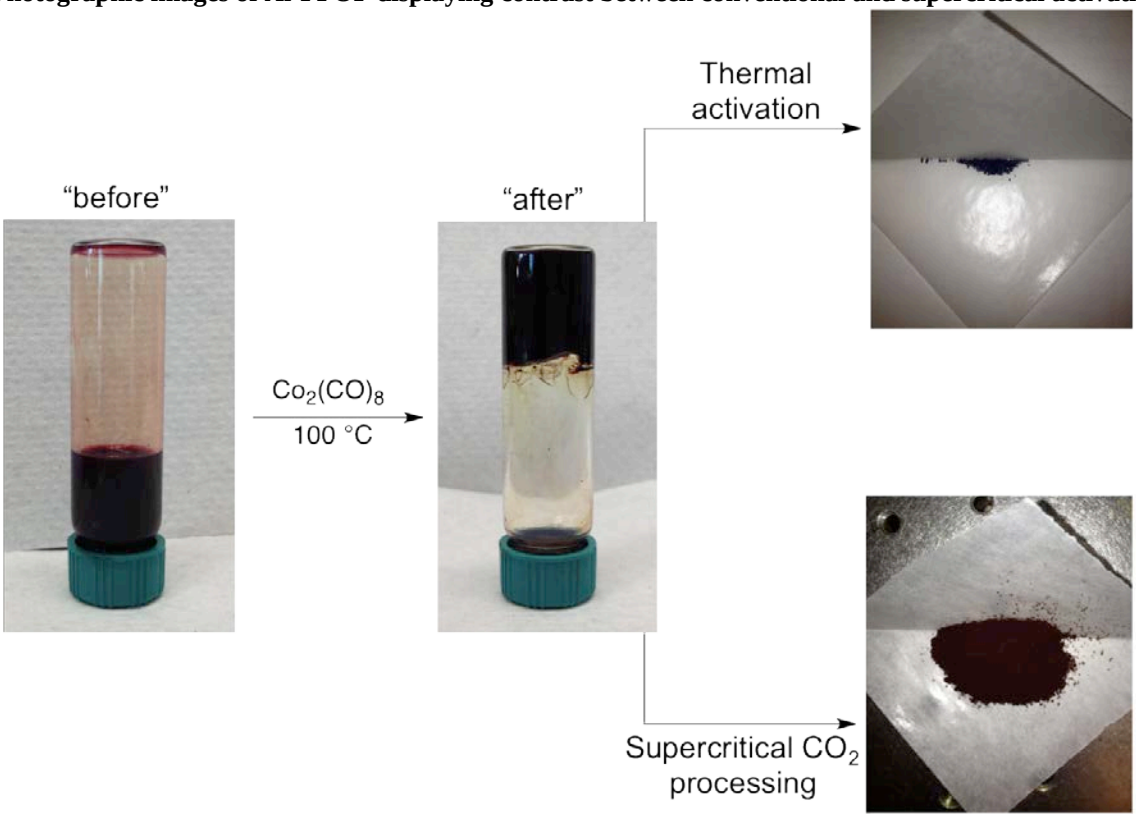

Figure S24. Left: photographic images of the Al-PPOP synthesis showing the gel-like materials that resulted at the end of the synthesis. Conventional activation affords a dense, brittle material (top right) while supercritical CO_2 processing affords a powdery, flocculent material (bottom right).

S19. Author contributions audit. R.K.T., O.K.F., J.T.H., and S.T.N. conceived the experiments presented herein. R.K.T and Y.S.K. synthesized all compounds with the exception of *tetrakis*(4-ethynylphenyl)methane, which was synthesized by M.H.W. R.K.T. carried out the characterization of all polymers, with exception to ICP-OES and methanol vapor isotherm experiments, which were conducted by M.H.W. R.K.T conducted the supercritical CO_2 activation, methanolysis experiments, recycling experiments, regeneration experiments, and Soxhlet extractions. O.K.F., J.T.H., and S.T.N. supervised the project. R.K.T. wrote the initial draft of the paper and received inputs and corrections from all co-authors. R.K.T. and S.T.N. finalized the manuscript.

S20. References.

(S1) Pangborn, A. B.; Giardello, M. A.; Grubbs, R. H.; Rosen, R. K.; Timmers, F. J. *Organometallics* **1996**, *15*, 1518-1520.
(S2) Totten, R. K.; Ryan, P.; Kang, B.; Lee, S. J.; Broadbelt, L. J.; Snurr, R. Q.; Hupp, J. T.; Nguyen, S. T. *Chem. Commun.* **2012**, *48*, 4178-4180.
(S3) Laha, J. K.; Dhanalekshmi, S.; Taniguchi, M.; Ambroise, A.; Lindsey, J. S. *Org. Process Res. Dev.* **2003**, *7*, 799-812.
(S4) Pandey, P.; Farha, O. K.; Spokoyny, A. M.; Mirkin, C. A.; Kanatzidis, M. G.; Hupp, J. T.; Nguyen, S. T. *J. Mater. Chem.* **2011**, *21*, 1700-1703.
(S5) Thamyongkit, P.; Lindsey, J. S. *J. Org. Chem.* **2004**, *69*, 5796-5799.
(S6) Lowell, S.; Shields, J. E.; Thomas, M. A.; Thommes, M. *Characterization of Porous Solids and Powders: Surface Area, Pore Size, and Density*; 4th ed.; Kluwer Academic: Dordrecht (The Netherland), 2004.